Global Land Cover Mapping using ADEOS-II/GLI Global Mosaic Data

Noriko Soyama
Center for Research and Development of Liberal arts Education, Tenri University, Nara, Japan
soyama@sta.tenri-u.ac.jp

Hiroko Tsujimoto
Laboratory of Nature Information Science, Department of Information and Computer Sciences,
Nara Women's University, Nara, Japan
hiroko@ics.nara-wu.ac.jp

Shinobu Furumi
KYOU SEI Science Center and Department of Information and Computer Sciences,
Nara Women's University, Nara, Japan
sfurumi@cc.nara-wu.ac.jp

Kanako Muramatsu
KYOU SEI Science Center and Department of Information and Computer Sciences,
Nara Women's University, Nara, Japan
muramatu@ics.nara-wu.ac.jp

Motomasa Daigo
Faculty of Economics, Doshisha University, Kyoto, Japan
mdaigo@mail.doshisha.ac.jp

Abstract: GLI aboard ADEOS-II is an optical sensor which observes reflected solar radiation and infrared radiation from Earth's surface with hyper-multi-channels, and it was expected to give us valuable information about the land cover and also vegetation state. Unfortunately, the operation of ADEOS II satellite has stopped on October 24 of 2003. We made a global land cover map using GLI global mosaic data sets which were acquired from April to October, in 2003. For hyper-multi-spectral data such as GLI, we have developed the universal pattern decomposition method (UPDM) which is sensor independent analysis method. By the UPDM, the multi-dimensional data of spectral reflectance are transformed into four coefficients which almost directly correspond to ground objects. Thus, we can find the feature of a pixel by comparing three coefficients values, and can calculate a vegetation index (VIUPD: Vegetation Index based on UPDM) with four UPDM coefficients. In this study, we apply categories of the Köppen Climate Classification for classifying global land cover. They are based on the annual and monthly averages of temperature and precipitation, and the scheme also takes into account the vegetation limits. The Köppen system recognizes five major climatic types, each category is further divided into sub-categories based on temperature and precipitation. By the UPDM, we calculate three coefficients and VIUPD values of sampling data sets which belong to each category of the Köppen Climate Classification, and defined the rule of classifying of land cover by examining the seasonal change of each VIUPD value. Our global land cover map roughly indicates same classification results as the global land cover map using NOAA-AVHRR by Wolfgang et al..
Keywords: land cover classification, Köppen Climate Map, Universal Pattern Decomposition Method(UPDM) ,ADEOS-II/GLI Global mosaic data.

1. Introduction

Global land cover mapping is important to study the natural alternation, such as global biogeochemical cycles, climate changing, estimation of net primary production. In recent years, global land cover map produced using satellite data has been on the increase. The global land cover map produced using data from the advanced very high resolution radiometer (AVHRR) by DeFries [3] is the first remote sensing research result. Subsequently, DeFries and Hansen et al. [4] produced a gland cover map using a decision tree classification from AVHRR data. In 2000, using data sets derived from AVHRR, Loveland et al. [7] produced a global land cover map at 1 km spatial resolution by unsupervised classification, and Hansen et al. [8] used a supervised classification to produce a map. However data sets derived from the AVHRR was limited to more accurately produce a global land cover map.

More recently, MODIS land cover [5] and GLC-2000 [6] produced global land cover data sets, and they have become available. MOIDS land cover is produced by Boston University using 1-km spatial resolution data sets of the continuous fields Moderate Resolution Imaging Spectrometer (MODIS). GLC-2000 is produced by Global Land Cover 2000 (GLC-2000) project, which is implemented by the Joint Research Center of the European Commission in partnership with more than 30 partner institutions around the world, using Satellite Pour l'Observation de la Terre (SPOT) VEGETATION 1-km satellite data. These were prepared using different data sources, classification systems and methodologies. In classification systems, GLC-2000 used a flexible classification system based on the Land Cover Classification System (LCCS) developed by Food and Agriculture Organization (FAO) and the United Nations Environment Programme (UNEP), on the other hand, MODIS land cover primarily used the International Geosphere Biosphere Prigramme (IGBP) classification system. In the comparative analysis of two global land cover data sets by Giri et al[1]., they are generally in agreement except a few classes.

In this paper, we show the global land cover map produced using the L2A_LC (v.180) global mosaic data of ADEOS-II/GLI provided by Japan Aerospace Exploration Agency (JAXA), and introduce the classification scheme of global land cover classification. The ADEOS-II/GLI provides hyper-multi-spectral data. We have developed an analysis algorithm, the universal pattern decomposition method (UPDM), which is sensor independent analysis method for hyper-multi-spectral data. By the UPDM, the multi-dimensional data of spectral reflectance are transformed into four coefficients which almost directly correspond to ground objects (i.e., water, vegetation and soil coefficients) and supplementary coefficient, and then we can find a feature of each pixel by comparing these coefficients values. We defined the classification scheme using the UPDM coefficients and the vegetation index based on the UPDM (VIUPD). Finally, we describe validation results of our global land cover map in comparison with MODIS land cover produced using Terra/MODIS by Boston University and global land cover map produced using NOAA-AVHRR by Wolfgang et al.

2. Data used in this study

The second Advanced Earth Observing Satellite (ADEOS-II) was designed to observe the earth multi-spectrally. Global Imager (GLI) aboard ADEOS-II is an optical sensor that observes reflected solar radiation and infrared radiation from earth's surface with 36-spectral channels ranging from 0.38 to 12.0 micrometers. GLI has several channels, whose wavelength is not included in the LANDSAT/TM spectral channels. Therefore, it is expected that GLI data give us valuable information about the land cover and also vegetation state. Unfortunately, the operation of ADEOS-II ceased operation on October 24 of 2003. However, it observed for about 7 months, from April to October 2003.

Table 1. Main characteristics of ADEOS-II GLI L2A_LC global mosaic data used in this study

Band Number	Central Wavelength [nm]	Spectral Width [nm]	Spatial Resolution [km]	Comment
5	460	10	1	ocean pigment
8	545	10	1	no ocean pigment
13	678	10	1	chl-a abs
15	710	10	1	aerosols
19	865	10	1	cloud opt. think., aerosols
24	1050	20	1	water/ice/snow
26	1240	20	1	water/ice/snow
28	1640	200	0.25	vegetation, soil moisture, ice phase
29	2210	220	0.25	cloud droplet size, soil moisture

Table 1 shows main characteristics of L2A_LC global mosaic data bands used in this study. L2A_LC data sets are composite over 16 days using 1 km spatial resolution data sets, and they are reduced the effect of clouds. We selected 9 bands in which light is not influenced strongly by water vapor and oxygen absorption, or aerosols in the atmosphere. The L2A_LC global mosaic data are comprised 56 areas. In this study, we used 48 areas from 60 degree north to 60 degree south latitude; one are includes 3600 pixels over 30 degrees in the horizontal, and 3600 pixels over 30 degrees in the vertical with map-projection of Equi-rectangular (EQR). We analyzed 13 composite data sets: April 7, April 23, May 9, May 25, June 10, June 26, July 12, July 28, August 13, August 29, September 14, September 30 and October 16. Since it

is hard to analyze huge data sets in which the total data size of all 48 areas is 7.5GB, we reduced data sets by sampling every twelfth pixel across each row and line of the data set.

3. Analysis method

To analysis global mosaic data sets, we used the Universal Pattern Decomposition Method (UPDM) and the vegetation index based on universal pattern decomposition (VIUPD). By the UPDM, the multi-dimensional data of spectral reflectance are transformed into four coefficients which almost directly correspond to ground objects (i.e., water, vegetation and soil coefficients) and supplementary coefficient. The VIUPD is a function of the linear combination of these coefficients.

3.1 UPDM (Universal Pattern Decomposition Method)

In the universal pattern decomposition method [10], a set of reflectance of n-bands for each pixel is decomposed by standard spectral patterns of water, vegetation, soil and the supplementary pattern coefficients of a yellow leaf as follows:

$$R(i) \rightarrow C_w \times P_w(i) + C_v \times P_v(i) + C_s \times P_s(i) + C_4 \times P_4(i) \quad , \tag{1}$$

where $R(i)$ is the reflectance of band i measured by satellite sensor for any pixel, and C_w, C_v, C_s and C_4 are the decomposition coefficients, and $P_w(i)$, $P_v(i)$, $P_s(i)$, and $P_4(i)$ are the standard spectral patterns of water, vegetation, soil, and the supplementary yellow-leaf pattern for band i (i indicates the sensor band numbers). The continuous of spectral pattern $(P_k(\lambda)(k = w, v, s, 4))$ was determined with spectral range from 350 nm to 2500 nm as follows,

$$P_k(\lambda) = \frac{\int d\lambda}{\int |R_k(\lambda)|\, d\lambda} \times R_k(\lambda) \qquad (k = w, v, s, 4) \quad , \tag{2}$$

where $R_k(\lambda)$ represents the continuous spectral reflectance of standard patterns $P_k(\lambda)$. The $P_4(\lambda)$ is defined using the yellow leaf residual as follows,

$$P_4(\lambda) = \frac{\int d\lambda}{\int |r_4(\lambda)|\, d\lambda} \times r_4(\lambda) \quad , \tag{3}$$

where $r_4(\lambda)$ is the residual value for a yellow leaf for the i band.

Fig.1 shows the normalized standard patterns of water, vegetation, soil and the yellow leaf supplement. They are calculated from the ground spectral measurement data of water, vegetation, soil and the supplement yellow leaf, respectively. The spectral region is selected where atmospheric transmittance exceeds 80%; from 371 nm to 900 nm, from 901 nm to 1100 nm, from 1191 nm to 1300 nm, from 1521 nm to 1750 nm and from 2081 nm to 2360 nm.

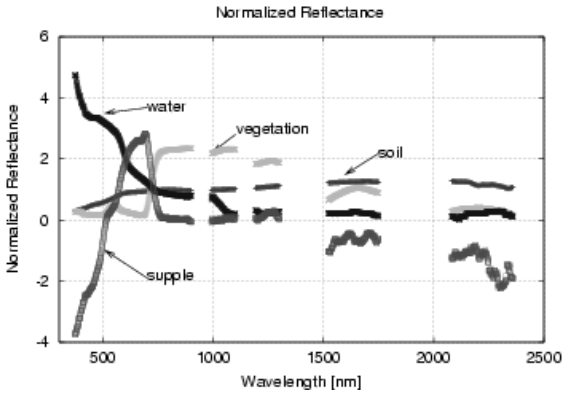

Figure 1. Normalized standard patterns of water, vegetation, soil and the yellow leaf supplement.

3.2 VIUPD (Vegetation Index based on Universal Pattern Decomposition)

The vegetation index based on universal pattern decomposition (VIUPD) can be used to examine vegetation amounts and vigor[11]. The VIUPD formula is given as follows,

$$VIUPD = \frac{C_v - 0.10 \times C_s - C_4}{C_w + C_v + C_s} \quad , \qquad (4)$$

where (C_w+ C_v+ C_s) represents the sum of total reflectance of all bands. The coefficient 0.10 with *Cs* was decided so that the average VIUPD of dead vegetation equals zero. For standard vegetation, the VIUPD value equals 1.

4. Classification scheme

4.1 Classes

In this study, in order to classify global land cover, we defined eight classes based on the Köppen Climate Classification. The Köppen Climate Classification System is the most widely used system for classifying the world's climates. Köppen divided the Earth's surface into climatic regions that generally coincided with patterns of vegetation and soils. The Köppen system recognizes five major climatic types, furthermore they are divided into sub-categories based on temperature and precipitation. We brought our classes (NWU class) into correspondence with Köppen's classes respectively (Tab 2.)

Table 2. NWU class definitions and Köppen classes.

Köppen classes	NWU classes
Tropical Moist Climates (Af) Tropical Monsoon (Am)	Tropical rain forest
Wet-Dry Tropical Climates (Aw)	Savanna
Dry Tropical Climate (Bw)	Desert
Dry Mid-latitude Climates (Bs)	Steppe
Humid Subtropical climates (Cfa,Cwa) Maritime Temperate climates (Cfb)	Broad leaf forest
Mediterranean Climate (Cs)	Sclerophyll forest
Boreal Climate (Df)	Coniferous forest
Highland Climate (H)	Woodless area

4.2 Sample Data for Analysis and classification definitions

In order to determine definitions of the classification, we examined the UPDM coefficients and the VIUPD values of pixels in each area classified by the Köppen Climate Classification System. As analysis areas, we selected four sites from areas classified by the Köppen Climate Classification System, furthermore, selected six pixels in every site. In order to examine annual change of each site, we prepared sample data sets consist of 13 composite global mosaic data sets respectively. Tab.3 shows a list of analysis sites: NWU classes, Köppen classes corresponding to NWU classes, site address, Latitude, Longitude. From results of calculating the UPDM coefficients and the VIUPD values of sample data sets, unfortunately, we found a number of lack data and inconsistent data with a feature of each class. Those data may be influenced by clouds. We selected consistent data with a feature of each class as closely as possible.

Fig.2 shows the VIUPD values and three UPDM coefficients indicated the most typical feature of each class. The x-axis is the date of composite global mosaic data sets and the y-axis is each value. From these figures, we find some feature of each NWU classes. The Tropical rain forest VIUPD is nearly 1.0 through all data. The Deserts' and Woodless areas' are nearly 0.0 through all date. The VIUPD values of Steppe roughly fix low. Other classes showed the seasonal change of the VIUPD. When the seasonal change of the VIUPD are examined, we could not use all composite global mosaic data, since there are lack data and inaccurate data under some influences of the atmosphere. As a pixel of the spring data, we selected a pixel whose VIUPD value is the highest from two data on April. The summer data and the autumn data were likewise selected from two data on August and September respectively. In view of the measure, Tropical rain forests', Broad leaf forests' and Coniferous forests' in summer are high, and Desert, Woodless', Savannas' and Steppes' are low.

Table 3. The list of analysis sites.

NWU classes	Köppen	Site	(Latitude, Longitude)	
Tropical rain forest	Af	Borneo(Sintang), Mindanao(General Santos)	(0., E 110.) (N 8., E125.)	
		Amazonia (Leticia, Tefe)	(S 3., W70.)	(S 3., W65.)
	Am	Amazonia(Roraima, Llanos)	(0., W60.)	(N 5., W70.)
		Fhilippines(Mindoro, Luzon)	(N 15., E120.)	(N 18., E122.)
Savanna	Aw	Brazil(Toncantins, Rondonia)	(S 10., W 50.)	(S 10., W60.)
		Upper Guinea(Nigeria, Sudan)	(N 10., W 16)	(N 10., E 10.)
Desert	Bw	Sahara Desert (Chad, Mali)	(N 20., E20.)	(N 20., 0.)
		Gibson Desert (Australia)	(S 23., E120.)	(S 25., E130.)
Steppe	Bs	Great Sandy Desert (Australia)	(S 18., E130.)	(S 33., E120.)
		Orsk (Kazakhstan) Kalahari Desert (Botswana)	(N 50., E60.) (S 20., E20.)	(S 25., E20.)
Broad leaf forest	Cfa	America(Memphis, Pampa)	(N 35., W90.)	(N 35., W100.)
		Japan(Kagoshima, Hyogo)	(N 32., E130.)	(N 35., E135.)
	Cfb	Europe(Vlore, Valencia)	(N 20., E20.)	(N 20., 0.)
		Europe(Limerick, Bayreuth)	(N 52., W10.)	(N 50., E10.)
	Cw	China(Yunnan, Henan)	(N 25., E100.)	(N 35., E115.)
		Zambia, Malawi	(S 15., E30.)	(S 10., E33.)
Sclerophyll forest	Cs	Europe(Meseta, Sardinia)	(N 40., W 5.)	(N 40., E 8.)
		Italy (Foggia), Greece(Thessalia)	(N 41., E16.)	(N 39., E22.)
Coniferous forest	Df	Russia(Ryazan, Khabarovsk)	(N 55., E40.)	(N 45., E130.)
		Canada(Brandon, The Pas)	(N 50., W100.)	(N 55., W100.)
Woodless area	H	Hinmalayas	(N 30., E90.)	(N 30., E100.)
			(N 30., E80.)	(N 35., E95.)

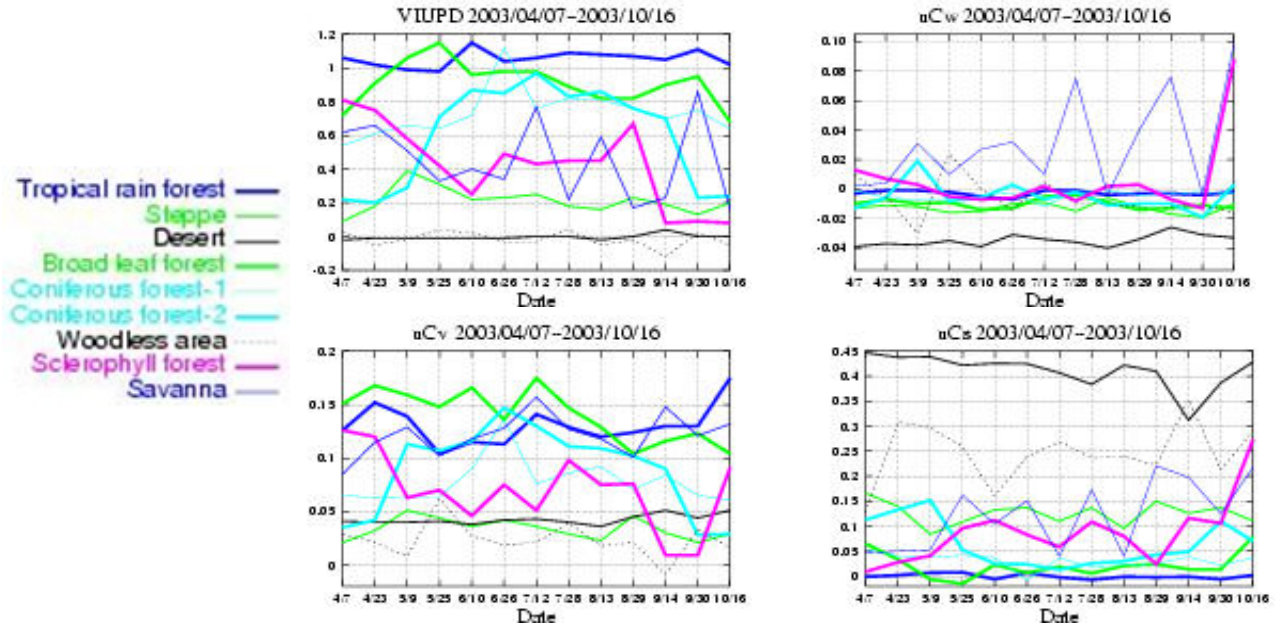

Figure 2. The VIUPD and three coefficients of sample data

As mentioned above, the C_w coefficients correspond to water objects, the C_v coefficients correspond to vegetation objects and the C_s coefficients correspond to soil objects. By comparing these values, we can find the feature of each pixel. We picked up the feature of each class from three UPDM coefficients graphs in Fig.2. The C_w coefficients of Desert class are much lower than other classes'. The C_v coefficients of Broad leaf forest are more than 0.1 through all season. In the case of Coniferous forest, the UPDM coefficients are varied by a situation of site. In high latitude area, the C_v coefficients in spring and autumn are lower than the C_s coefficients. The C_v coefficients of Steppe are also lower than the C_s coefficients in spring and autumn, however, the VIUPD values in summer are lower than Coniferous forest classes'. In the case of Sclerophyll forest, the VIUPD values in summer are lower than Broad leaf forest classes', and the VIUPD values in autumn are lower than Savannas'.

Table 4. The classification rules.

<table>
<tr><th colspan="2">Spring(April)</th><th colspan="2">Summer(August)</th><th>Autumn (September)</th><th>NWU Classes</th></tr>
<tr><td rowspan="2">VIUPD＜0.15</td><td>uCv-uCw>=0.03</td><td colspan="2" rowspan="2">VIUPD＜0.15</td><td rowspan="2">VIUPD＜0.15</td><td>Desert</td></tr>
<tr><td></td><td>Woodless area</td></tr>
<tr><td colspan="2">VIUPD>=0.9</td><td colspan="2">VIUPD>=0.9</td><td></td><td>Tropical rain forest</td></tr>
<tr><td colspan="2" rowspan="4">uCv>=uCs</td><td rowspan="2">VIUPD>=0.65</td><td>uCv＜0.1</td><td rowspan="2"></td><td>Coniferous forest</td></tr>
<tr><td></td><td>Broad leaf forest</td></tr>
<tr><td colspan="2" rowspan="2"></td><td>VIUPD>=0.1</td><td>Savanna</td></tr>
<tr><td></td><td>Sclerophyll forest</td></tr>
<tr><td colspan="2" rowspan="2">uCv＜uCs</td><td colspan="2"></td><td rowspan="2">uCv＜uCs</td><td>Steppe</td></tr>
<tr><td colspan="2">VIUPD>=0.8</td><td>Coniferous forest</td></tr>
</table>

4. Global land cover map and validation

Fig3. shows the map of final product except areas above 60 degrees north latitude. Since noises were found in most areas above 60 degrees north latitude in GLI global mosaic data sets used in this study, we compared sites except those areas. The NWU global land cover map is roughly in agreement with NOAA-AVHRR by Wolfgang, et al.[9]. Wolfgang's map (NOAA map) is a simplified map of natural vegetation inferred from NOAA-AVHRR satellite imagery using an empirical algorithm, and the classification system consists of six classes; Desert, Savanna, Grassland, Deciduous forest, Mixed forest and Evergreen forest. Crops and natural vegetation are excluded. In order to compare two global land cover maps, we need to translate from classes of the NOAA map to the NWU classes except Dessert class and Savanna class. We consider equivalent classes of the NOAA map as follows. The grassland class is translate to Steppe class, the evergreen forest class is Tropical rain forest class, the mixed forest class is Coniferous forest class and Sclerophyll forest class, the deciduous forest class is Broad forest class. the NOAA map classification system have no equivalent class to Woodless area class.

In Desert class areas, good agreement between two maps is observed, except Australia and South Africa. Our classification scheme can found a few Savanna class in the Australia, most of savanna areas detected by NOAA map are Desert, Broad forest and Sclerophyll forest in our map. Savanna areas in Africa are also fewer than NOAA map. Savanna area in NWU map may be not well derived for inaccurate sample data sets. It was hard to look up sample data from Savanna area, since many lack data and inaccurate data were found in Savanna area. But for all that, in South America, good agreement between two maps is shown. Steppe class is good agreement except areas in the north high latitude and tundra climate area in Asia. Tundra area in Asia of NOAA map are classified into Savanna. It's probably because NOAA map have no Woodless class. Broad forest class and Coniferous forest class are good agreement respectively. Most of Japan of NWU map were classified into Broad leaf forest class. As for NOAA map, all of south area were mixed forest class, and north area were classified into deciduous forest class despite north area in Japan are Coniferous forest.

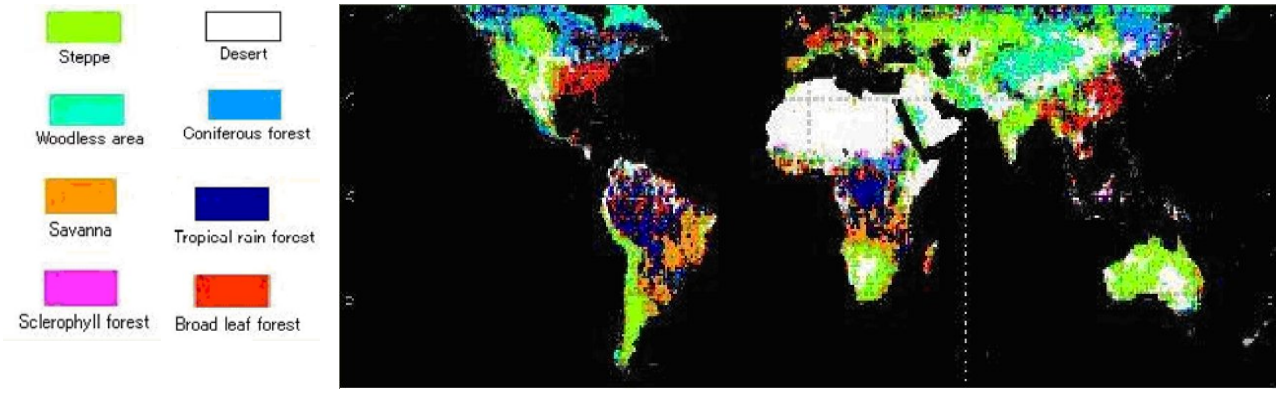

Figure 3. Final classification product (NWU global land cover map)

The comparison of our global land cover map (NWU land cover) to Hansen's MODIS land cover map (MODIS land cover) is shown in Tab.5. In this comparison, we consider that Sclerophyll forest is equivalent to Shrublands of MODIS land cover, since Shrublands is determined as 'Land with woody vegetation less than 2m tall and with shrub canopy cover between 10% and 60% , or >60%.' in MODIS land cover. Wetlands area is not determined in our classification system, however, NWU land cover map are good agreement with MODIS land cover map except Savanna, Sclerophyll forest and Steppe of NWU land cover. As mentioned above, it is hard to find sample data of Savanna class, since there are lack data and inaccurate data under some influences of the atmosphere. The results of classification for Savanna may be inaccurate.

Table 6. The comparison between NWU land cover and MODIS land cover.

<table>
<tr><td colspan="3">MODIS land cover (%)</td><td colspan="3">NWU land cover (%)</td></tr>
<tr><td colspan="2" rowspan="3">Forest</td><td rowspan="3">25.0</td><td>Tropical rain forest</td><td>4.1</td><td rowspan="3">24.2</td></tr>
<tr><td>Broad leaf forest</td><td>10.3</td></tr>
<tr><td>Coniferous forest</td><td>9.8</td></tr>
<tr><td colspan="2" rowspan="2">Shrublands</td><td rowspan="2">36.2</td><td>Savanna</td><td>10.6</td><td rowspan="2">28.7</td></tr>
<tr><td>Sclerophyll forest</td><td>18.1</td></tr>
<tr><td>Grasslands</td><td>8.4</td><td rowspan="3">23.7</td><td colspan="2" rowspan="3">Steppe</td><td rowspan="3">30.9</td></tr>
<tr><td>Croplands</td><td>11.5</td></tr>
<tr><td>Cropland / natural vegetation</td><td>3.8</td></tr>
<tr><td>Urban</td><td>0.2</td><td rowspan="2">14.6</td><td colspan="2" rowspan="2">Desert
Woodless area</td><td rowspan="2">16.2</td></tr>
<tr><td>Barren</td><td>14.4</td></tr>
<tr><td colspan="2">Wetlands</td><td>0.5</td><td colspan="2"></td><td></td></tr>
</table>

4. Conclusions

We tried to produce global land cover map using ADEOS-II GLI global mosaic data sets. Although ADEOS-II was operated for a short term unfortunately, we could obtain data sets for about 7 months, from April to October 2003. These data sets may imply the season change of the northern hemisphere and may give much useful information to examine each feature of land cover type. We analyzed these data sets using the UPDM and examined four coefficients and the VIUPD values. Although several lack data exist, we can find the feature of each class and determined classification scheme. Our global land cover map is roughly in agreement with products using NOAA-AVHRR by Wolfgang et al., and some agreement between NWU map and MODIS land cover map were only observed. It is hard to produce the global land cover map, since data sets used in this study have many noises and lack data. However, GLI mosaic data sets produced by next version will reduce these problems and we expect to detect each pixel more exactly by new data sets.

In the next work, we are going to investigate the anthropogenic area; paddy, cropland, built-up area, etc, and we would like to produce useful information for estimating the global terrestrial net primary production.

Acknowledgement

This work was supported under the ADEOS-II/GLI project by Japan Aerospace Exploration Agency (JAXA). We thank World Wide Business Center, Doshisha University Academic Frontier Project.

References

[1] Chandra Giri, Zhiliang Zhu and Bradley Reed , 2005, "A comparative analysis of the Global Land Cover 2000 and MODIS land cover data sets", *Remote Sensing of Environment*, 94: 123-132

[2] Daigo, M., Ono, A., Fujiwara, N., and Urabe, R., 2004. "Pattern decomposition method for hyper-multi-spectral data analysis," *International Journal of Remote Sensing*, 25(6): 1153-1166.

[3] DeFries, R., S., Townsend, J. G. R., 1994, "NDVI derived land cover classifications at a global scale.", *International Journal of Remote Sensing* , 5:3567-3586.

[4] DeFries, R., S., Hansen, M., C., Townsend, J. G. R., Sohlberg, R., 1998, "Global land cover classifications at 8 km resolution: the use of training data derived from Landsat imagery in decision tree classifier.", *International Journal of Remote Sensing* , 19:3141-3168.

[5] Friedl, M.A., McIver, D.K., Hodges, J.C.F., Zhang, X. Y. Muchoney, D., Strahler, A. H., et al. 2002, "Global land cover mapping from MODIS: algorithms and early results.", *Remote Sensing of Environment* , 83(1-2):287-302.

[6] Fritz, S., Bartholome, E., Belward, A., Hartley, A., Stibig, H.-J., Eva, H., et al. 2003, "Harmonization mosaicking, and production of the Global Land Cover 2000 database.", Ispra, Itary : Joint Resarch Center(JRC).

[7] Loveland, T.R., & Reed, B.C., Brown, J.F., Ohlen, DO.O., Zhu, Z., Yang, L., Merchant, J.W., 2000, "Development of a global land cover characteristics database and IGBP DISCover from 1 km AVHRR data.", *International Journal of Remote Sensing* , 21(6-7):1303-1365.

[8] Hansen, M., C., DeFries, R., S., Townsend, J. G. R., Sohlberg, R., 2000, "Global land cover classification at 1 km spatial resolution using a classification tree approach" , *International Journal of Remote Sensing*,vol. 21, no. 6 & 7, 1331–1364.

[9] Wolfgang Cramer, Bondeau A, Woodward FI, Prentice IC, Betts RA, Brovkin V, Cox PM, Fisher V, Foley J, Friend AD, Kucharik C, Lomas MR, Ramankutty N, Sitch S, Smith B, White A & Young-Molling, "C 2001 Global response of terrestrial ecosystem structure and function to CO2 and climate change: results from six dynamic global vegetation models", *Global Change Biology*, 7(4):357-373.

[10] Zhang, L. F., Furumi, S., Murumatsu, K., Fujiwara, N., Daigo, M., and Zhang, L. P., 2004. "Sensor-independent analysis method for hyper-multi spectra based on the pattern decomposition method" , *International Journal of Remote Sensing*, (submitted).

[11] Zhang, L. F., Furumi, S., Murumatsu, K., Fujiwara, N., Daigo, M., and Zhang, L. P., 2004. "A New Vegetation Index Based on the Universal Pattern Decomposition Method" , *International Journal of Remote Sensing*, (submitted).